Local properties of filter cakes formed from pH-adjusted bauxite residue slurries

Kinnarinen Teemu, Theliander Hans, Häkkinen Antti, Mattsson Tuve

Local properties of filter cakes formed from pH-adjusted bauxite residue slurries

Teemu Kinnarinen[a*], Hans Theliander[b], Antti Häkkinen[a], Tuve Mattsson[b]

[a] LUT School of Engineering Science, Lappeenranta University of Technology,
Lappeenranta, Finland
[b] Department of Chemistry & Chemical Engineering, Chalmers University of Technology,
Gothenburg, Sweden
*Corresponding author: Teemu Kinnarinen, P.O. Box 20, 53851 Lappeenranta, Finland (*teemu.kinnarinen@lut.fi*)

Abstract

Solid-liquid separation of bauxite residue is a topical issue in the alumina industry, not least due to the great quantity and problematic properties of this highly alkaline residue. The objective of this contribution is to provide deeper knowledge about the solid-liquid separation of pH-adjusted (pH 11) bauxite residue by investigating the local filtration properties of filter cakes produced with a piston press. Two bauxite residue samples having different particle size distribution were investigated. Measured local data of the hydrostatic pressure and solidosity was used together with flow rate data to calculate local specific filtration resistance as well as compressibility data. For the investigated pressure range (0.2 to 2 MPa) it was found that the residue formed slightly/ moderately compressible filter cakes with a specific cake resistance between $5 \cdot 10^{11}$ to $1.5 \cdot 10^{12}$ m/kg. The sodium recovery and final cake solidosity were strongly dependent on the applied pressure, but only to a minor extent on the particle size reduction obtained by the applied mechanical treatment. The filter cakes formed from the mechanically treated samples did, however, display a somewhat higher pressure dependence for the local specific filtration resistance compared to the non-ground samples.
Keywords: Bauxite residue; Red mud; Filtration; Separation; Filter cake; Local properties

1. Introduction

Safe disposal of bauxite residue is a huge challenge for the alumina industry. For each ton of alumina produced, approximately 1-1.5 tons of bauxite residue are generated [1,2], in some cases even more [3,4]. Bauxite residues have high alkalinity, buffering capacity and electrical conductivity, and they contain large quantities of dissolved metal ions, especially sodium [5,6]. The mineralogical composition of the solid phase varies depending on several factors, but most typically Fe_2O_3, $FeOOH$, SiO_2, TiO_2, CaO and sodium aluminium silicates as desilication products are present at high amounts [7-9]. Due to the adverse properties and the excellent availability of bauxite residues, several utilization methods have been proposed in the literature, although the utilization in industrial scale is still scarce. Potential future applications can be found e.g. in the construction industry [10,11], various fields of metallurgy [12,13], agriculture [14], production of ceramics, pigments and catalysts [15], as well as treatment of contaminated liquids [1]. Practical challenges are caused by the chemical composition, for instance by the Cl content, which is often too high for cement production [16].

Disposal of bauxite residue in the alumina industry is typically performed after thickening the residue slurry in a countercurrent thickening/washing train at a total solid content of < 60 wt.% [17], retaining the residue in pumpable form for transport to the disposal area (dry stacking). Alternatively, disposal is performed after increasing the total solid content by pressure filtration to approximately 70-75 wt.% [18-21], and in this case the residue is transported to the disposal area as compact cakes (dry cake disposal). Currently, these two treatment and dry disposal methods are the most recommendable options for bauxite residues, unlike a couple of decades ago, when alumina refineries relied on marine discharge and lagooning [21]. The main reason for the implementation of dry disposal methods is the toxicity of bauxite residue to the environment [17] and the apparent risks caused for the local environment by large disposal ponds [22]. Neutralization of the residue prior to disposal by using for instance seawater, acids or CO_2 may reduce the risks caused by its high alkalinity further [23]. Additionally, gypsum may be applied as a surface layer at the dry disposal areas of the residue to facilitate revegetation [24].

The filtration behavior of slurries is today still normally investigated by examining average filtration properties, followed by modeling based on these average properties by using the classical filtration equation based on Darcy's work [25]. However, this approach has several limitations. For material that forms compressible filter cakes, i.e. cakes where the local cake structure varies over the height of the filter cake, these kinds of average measurements and models are not sufficient. Furthermore, investigation of local properties can be very valuable when detecting cake cracking behavior, skin formation and other changes in the cake structure and cake resistance [26]. In the literature, several examples of studies of local filtration properties can be found. Local hydrostatic pressure has been investigated by using pressure probes in different configurations (e.g. [27-30]), while local solidosity of filter cakes or sediments has been measured with different techniques, including cake dissection [31,32], nuclear magnetic resonance [33,34], conductivity measurements [27,28], and γ and x-ray attenuation [30,35,36].

In spite of the emerging research activity on the topic of bauxite residue filtration [18-20,37,38] no information is available about the local filtration properties of bauxite residues. The purpose of this paper is to investigate how the local properties of filter cakes formed from pH-adjusted bauxite residue slurry are influenced by particle size and filtration pressure. The local cake properties are investigated in-situ by using a piston press equipped with pressure capillaries to measure the local hydrostatic pressure within the cake, and a γ-ray attenuation system used for measuring the local solidosity at certain heights of the cake. The final properties of the filter cake, including e.g. the residual sodium and moisture contents and the average solidosity, are also discussed.

2.   Materials and methods

2.1.   Slurry preparation

Bauxite residue slurry of industrial origin was used in the filtration experiments. At the refinery, the sample was taken from the underflow pipe of the last thickener of the bauxite residue washing train. The primary sample (V = 0.3 m^3) was kept mixed overnight in a large mixing tank. A significantly smaller sub-sample of approximately 15 dm^3 was taken from the mixing tank. Part of the sample was then ground in a vertical stirred media mill (Vollrath-Salomix, P = 0.75 kW):

rotation speed = 700 rpm, grinding time = 30 min, mass of slurry = 4 kg, vessel volume = 5 dm³, mass of beads = 2 kg, diameter of beads = 2 mm. Glass beads were used as the grinding media. The objective of experiments with ground samples was to investigate the influence of particle size distribution on the filtration properties. The aim was to obtain a better understanding of the effect of particle size distribution on the specific cake resistance, solidosity and compressibility. These experiments were considered important, because the particle size distributions may vary significantly in industrial treatment of bauxite residue solids. After grinding, the beads were separated from the slurry by pouring the slurry through a sieve with an opening 1.4 mm in diameter. The dimensions of the stirred media mill have been described in detail by Kinnarinen et al. [39].

The density of the slurry was determined by taking a certain volume of slurry in a graduated glass cylinder and measuring its mass. The slurry sample was dried in an oven at 105 °C to determine the total solids content. The concentration of total dissolved solids in the liquid phase of the slurry was measured by drying the sample of centrifuged supernatant in the oven at 180 °C to dryness. A Metrohm 859 thermometric titrator was applied for the determination of the total caustic, comprising the free hydroxyl ion content and one mol OH^- per mol aluminate. The particle size distributions of the original and ground slurries were measured with a Malvern Mastersizer 3000 laser diffraction analyzer. The main properties of the slurry are presented in Table 1.

Before the filtration experiments, the pH of the slurry was reduced to pH 11 by using hydrochloric acid. To adjust the pH, a slurry sample with a mass of 0.830 kg was poured in a 3-liter jacketed feed tank, which was cooled by passing 10 °C water through the jacket. The required HCl (37 % solution) dosage was 0.095 kg_{HCl} / kg_{slurry}, and the addition rate was 0.1 dm³/min. The slurry was kept mixed during the pH reduction. Due to the exothermic neutralization reactions, the temperature increased temporarily to approximately 40 °C. Mixing and cooling were continued until the slurry temperature decreased to 22 °C. The pH reduction increased the viscosity of the slurry, so the slurry had to be diluted by adding 0.1 kg water per 1 kg of slurry, in order to enable fluent feed into the filter cell.

Table 1.　　　Properties of the diluted bauxite residue slurry at pH 11, 20 °C.

Slurry (-)	ρ_{slurry} (kg m⁻³)	Total solids (g kg⁻¹$_{slurry}$)	TDS* (g kg⁻¹$_{liquid}$)	TC** (g kg⁻¹$_{liquid}$)	D_{10} (µm)	D_{50} (µm)	D_{90} (µm)	D[3,2] (µm)	D[4,3] (µm)
Original	1400	417	99	2.2	1.5	18	138	4.2	47
Ground					1.4	3.7	18	2.0	8.8

*Total dissolved solids in liquid phase
**Total caustic as Na_2O with respect to liquid phase

In addition to the properties presented in Table 1, the density of the solid phase in the slurry (ρ_s = 2846 kg m⁻³) was measured by a gas pycnometer (Micromeritics AccuPyc II 1340). The measurements with the pycnometer were performed after the sample had been dried to total dryness at 105 °C. The volumetric fraction of suspended solids, i.e. solidosity, in the diluted slurry at pH 11 was approximately 20 %. This is in the same range as the solidosities reported for clarifier underflows of various refineries by Usher [40].

2.2. Filtration equipment

The filtration experiments were performed in a test filter apparatus comprising a pneumatically driven (Bosch Rexroth AB, cyl167/200/130) piston press designed for investigating local filtration properties during cake formation, expression and washing. The piston position was measured with a position sensor (Temposonic EP-V-0200M-D06-1-V0). The cylindrical filter cell had the total height of 17.5 cm with the diameter of 6 cm, whereof the lower part consisted of an 11.5 cm high Plexiglas cylinder that enabled both low γ-attenuation as well as visual observation. The bottom of the cell consisted of a perforated plate that served as a support for the filter medium (Munktell grade 5 filter paper). Eight capillary tubes, mounted through the bottom plate with apertures (0.6 mm in diameter) perpendicular to the flow direction and connected to pressure transducers (Kristal Instrument AG, maximum error 10 kPa) enabled measurements of local hydrostatic pressures at positions of 12, 9, 7, 5, 3, 2, 1, 0.5 mm from the bottom plate. The capillaries were rinsed with pure water prior to each experiment to ensure that the tubes were completely water filled before the filtration was initiated. This procedure cleaned the tubes and displaced air that would compress during the experiment and allow slurry to enter the tubes resulting in a build-up of solids and consequent plugging. The filtrate leaving the cell was collected and weighed on a scale (Mettler Toledo SB 32000).

The attenuation of an individual slice of the filter cell was investigated *in-situ* by using a collimated ^{241}Am γ-source, 10^9 Bq in tandem with a detector, both being mounted on a movable rack. The γ-source as well as the detector were well shielded, with the exception of a slit 24 mm wide and 3 mm high at the source and 24 mm wide and 1 mm high at the detector. A more detailed description of the apparatus can be found in the literature [30].

2.3. Experimental procedure

The sealed lid of the slurry tank was closed, and the top inlet of the tank was connected to a compressed air pipeline set to 20 kPa to feed the slurry into the filter cell, connected to the tank with a hose. Immediately after filling the cell completely, the feed valve was closed and the piston was released to start the filtration at the preset pressure. The experiments were carried out in arbitrary order according to the plan presented in Table 2. The filtration pressure was set by regulating the pressure to the pneumatic pressure cylinder (reported as target filtration pressure in Table 2) and the individual experiments are referred to using these pressure levels. The filtration pressure was also measured by the pressure transducers connected to the capillary tubes at position where no cake had yet formed in the beginning of the filtration (reported as measured pressure in Table 2). The later value has been used in all calculations due to the higher accuracy of these pressure transducers. Influence of frictional loses between the piston and the filter cell wall are also eliminated when using this method for estimation of the filtration pressure.

Table 2. Filtration experiments performed.

Test number (-)	Filtration pressure (target) (MPa)	Filtration pressure (measured) (MPa)	Type of slurry (-)
1	0.2	0.17	Original
2	0.6	0.59	Original
3	1.2	1.26	Original
4	2	2.11	Original
5	0.2	0.15	Ground
6	0.6	0.63	Ground
7*	1.2	1.24	Ground
8	2	2.18	Ground

Repeated for solidosity measurement at h = 5, 26, and 36 mm

In the tests, both filtration (cake build-up) and expression were performed. The cake expression was continued until virtually constant solidosity was reached, according to the measurement system introduced below in Section 2.3.1. Depending on the pressure, the time required for this varied from about two hours to overnight expression. For instance, when the pressure difference was 2 MPa (Test 4), the height of the cake changed only by 0.3 mm between 5000 and 7000 s, corresponding to 0.4 % of the average cake height during that time.

2.3.1. Data collection

The piston position, filtrate weight and local hydrostatic pressures were collected with a data acquisition device and recorded every two seconds by using Labview (National Instruments, USA). The local attenuation of the filter cake was investigated 12 mm from the bottom of the filter cell; the total number of counts collected by the detector in the 33-83 keV range was recorded for every minute by using Maestro data recording software. Evaluation of the validity of the measurement techniques for predicting local cake characteristics can be found in Johansson and Theliander [41].

2.3.2. Cake analyses

The filter cakes were dried at 105 °C to complete dryness to determine the solid contents. The dried cakes were homogenized by crushing, reslurried in water to a liquid/solid ratio of 9/1, and the liquid was analyzed for soluble sodium with flame atomic absorption spectroscopy F-AAS (Thermo Scientific iCE 3400 AA).

3. Calculations and data processing

The determination of local solidosity from the collected attenuation data was based on the Beer-Lambert law (Eq. 1):

$$-\ln\frac{n_\gamma}{n_{\gamma,0}} = \mu_{\gamma,l}d_\gamma + (\mu_{\gamma,s} - \mu_{\gamma,l})d_\gamma\Phi \tag{1}$$

where n_γ is the number of counts for the filter cell with cake, $n_{\gamma,0}$ is the number of counts for an empty cell, $\mu_{\gamma,l}$ and $\mu_{\gamma,s}$ are the attenuation coefficients for the liquid and solid phases, respectively, d_γ is the inner diameter of the filter cell, i.e. the path of the γ-radiation in the cell, and Φ is the local solidosity, i.e. the volumetric fraction of suspended solids in the cake at the height of measurement. The attenuation coefficients of the solid and liquid phase were determined, by direct measurement on the filtrate and the expressed cake, to be 136.8 and 22.04 m^{-1}, respectively.

The average solidosity, Φ_{av}, of each filter cake was calculated from Eq. (2):

$$\Phi_{av} = \frac{V_{ss}}{V_c} \tag{2}$$

where V_{ss} is the volume of suspended solids, i.e. the remainder of $V_{total\ solids}$ - $V_{dissolved\ solids}$ in the overall cake, and V_c is the total volume of the cake.

The local specific cake resistance, α, was calculated by using the combination of a modified Darcy equation [42] and the relationship between permeability and specific resistance to filtration. After assuming that the velocity for the solid material in the cake is much smaller than the liquid velocity, which applies during the filtration stage, the equation becomes [43]:

$$\alpha = -\frac{1}{v\mu\rho_s\Phi}\frac{dp_L}{dz} \tag{3}$$

where v is the superficial flow velocity of the liquid in the z-direction, μ is the viscosity of the filtrate, ρ_s is the density of solids, p_L is the hydrostatic pressure and z is the distance from the filter medium. The expression stage was not considered due to the above-mentioned assumption of a negligible relative solid velocity. The hydrostatic pressure gradient dp_L/dz was calculated by using the values measured at the heights of 9 and 12 mm, and the local solidosity was measured at the height of 12 mm. The solid compressive pressure p_s and the hydrostatic pressure p_L can be related to each other according to Eq. (4), presented in the literature [44]:

$$dp_s = -dp_L \tag{4}$$

The reciprocal form of the Darcy equation was used for the calculation of the average specific cake resistance:

$$\frac{dt}{dV} = \alpha_{av}\mu c \frac{V}{A^2 \Delta p} + \frac{\mu R_m}{A\Delta p} \tag{5}$$

where t is time, V is the filtrate volume, c is the mass of solids in the filter cake per volume of filtrate, A is the filtration area, Δp is the filtration pressure, and R_m is the resistance of the filter medium and α_{av} is the average specific cake resistance defined according to Eq. (6):

$$\frac{1}{\alpha_{av}} \equiv \frac{1}{p_c} \int_0^{p_c} \frac{1}{\alpha} dp_s \tag{6}$$

where p_c is the pressure drop over the cake.

The cake compressibility was evaluated by using semi-empirical constitutive relationships Eqs. (7) and (8) [45]:

$$\alpha = \alpha_0 \left(1 + \frac{p_s}{p_0}\right)^n \tag{7}$$

where p_s is the solid compressive stress, and α_0, p_0 and n are parameters.

$$\Phi = \Phi_0 \left(1 + \frac{p_s}{p_0}\right)^\beta \tag{8}$$

where Φ_0, p_0 and β are parameters. Parameter Φ_0 can be interpreted to represent the estimated solidosity at zero compressive pressure.

By combining Eqs. (6) and (7) the average specific filtration resistance could be related to the parameters of the constitutive relationship:

$$\alpha_{av} = \alpha_0 \frac{(1-n)\frac{p_c}{p_0}}{\left(1+\frac{p_c}{p_0}\right)^{1-n}-1} \tag{9}$$

4.   Results and discussion

4.1.   Filtration curves

The filtrate accumulation curves for the original and ground bauxite residue slurry at the different filtration pressures are presented in Fig. 1a, where it can be seen that the total volume of liquid separated from the slurry depends strongly on the filtration pressure. A low total volume of filtrate collected during an experiment reflects a final cake with lower final solidosity. In all cases, there is a slight difference between the filtration curve of the original (solid line) and the ground (dashed

line) slurry, the non-ground samples being faster to filter. The relatively modest difference between the non-ground and ground material may be partly due to the fact that the increase of the smallest particle size fraction was relative small, i.e. the increase of surface contact area between the solids and the flowing liquid was limited. The narrower size distribution, which was the result of grinding, may also have had a positive effect on the filtration resistance.

The inversed filtrate flow rate (dt/dV) is presented as a function of filtrate volume in Fig. 1b. The data with fitted lines constitutes the linear part of the data. The beginning of the expression period, which can be clearly observed in the strong change of the slope of the data, is shown in Fig. 1b as well.
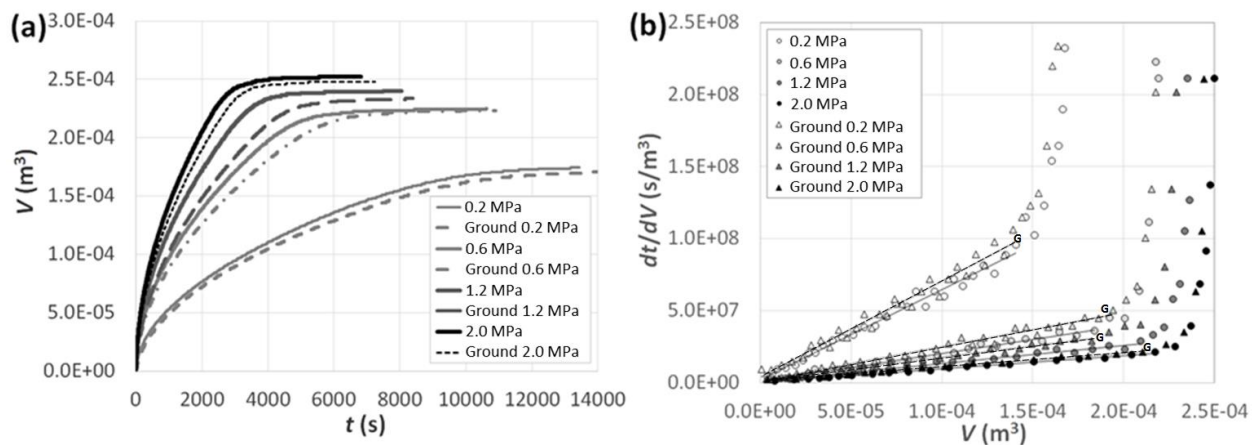

Figure 1.　(a) Volumetric accumulation curves of filtrate for the experiments. The solid and dashed line represent the original and ground samples, respectively. (b) The dt/dV vs. V curves with fitted lines for the linear parts of the data for the same experiments (G denotes a ground sample).

4.2. Average specific cake resistance

The average specific cake resistance, α_{av}, for each experiment (Fig. 2) was calculated according to Eq. (5), using the filtration data corresponding to the linear region displayed in Figure 1b. Fig. 2 shows that the average specific cake resistances were relatively high, and they increased with the piston pressure, displaying a compressible behavior. The grinding of the slurry had a slight influence on α_{av}: the mechanical treatment increased the filtration resistance, which is in line with a higher particle surface area. In general, the average specific cake resistances were within a typical range for pressure filtration operations, which means that vacuum filters would not be suitable for the investigated slurry. The compression behavior of the cakes is discussed with respect to the local data in Section 4.6 of this paper. Kinnarinen et al. [18] report α_{av} of approximately $6.0 \cdot 10^{11}$ m/kg for a bauxite residue with relatively similar characteristics to the original slurry (Table 1) without pH adjustment (pH = 13.2) at 0.6 MPa, which is on the same order as the values obtained in this study at the same pressure difference. The specific cake resistance may vary depending on the sample, for instance, Rousseaux et al. [20] report α_{av} of about $1.8 \cdot 10^{12}$ m/kg obtained in pilot-

scale test work without pH adjustment at 0.6 MPa. Rousseaux et al. [20] do not report the particle size distribution of the test slurry, but conclude that the filterability of the slurry was very poor.
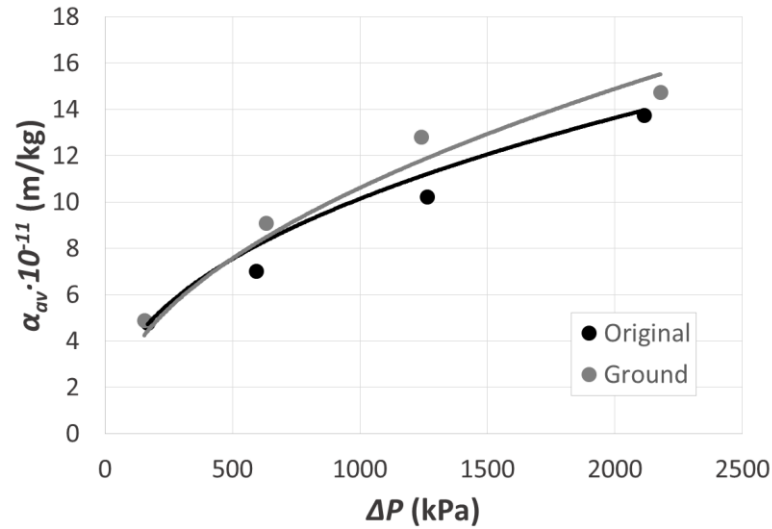

Figure 2.   Average specific cake resistance of original and ground slurries calculated by using Eq. (5). Lines represents the average specific filtration resistance based on Eq. (9) fitted to average and local data as described in section 4.6.

4.3. Moisture and sodium contents of filter cakes

The final moisture contents of the filter cakes were significantly reduced with the increasing filtration pressure, as shown in Fig. 3. The effect of the grinding treatment was not significant in the case of residual moisture and sodium contents. Increasing the piston pressure from 0.2 to 2 MPa resulted in a reduction of the moisture content of the cake from approximately 40 wt.% to 30 wt.%, corresponding to an increase in the average solidosity from 0.32 to 0.44. However, approximately half of the reduction of the moisture content took place between 0.2 and 0.6 MPa already. The residual sodium concentrations in the cakes decreased from about 25 $g_{Na}/kg_{dry\ cake}$ to about 15 $g_{Na}/kg_{dry\ cake}$. These sodium concentrations corresponded to sodium recoveries of 49 and 70 %, respectively. Sodium recovery is an important measure of filtration performance, describing what percentage of the water-soluble sodium fed into the filter is removed from the slurry with the filtrate. All results in Fig. 3 are reported for cakes compressed until reaching terminal solidosity, i.e. until the movement of the piston was completely stopped.
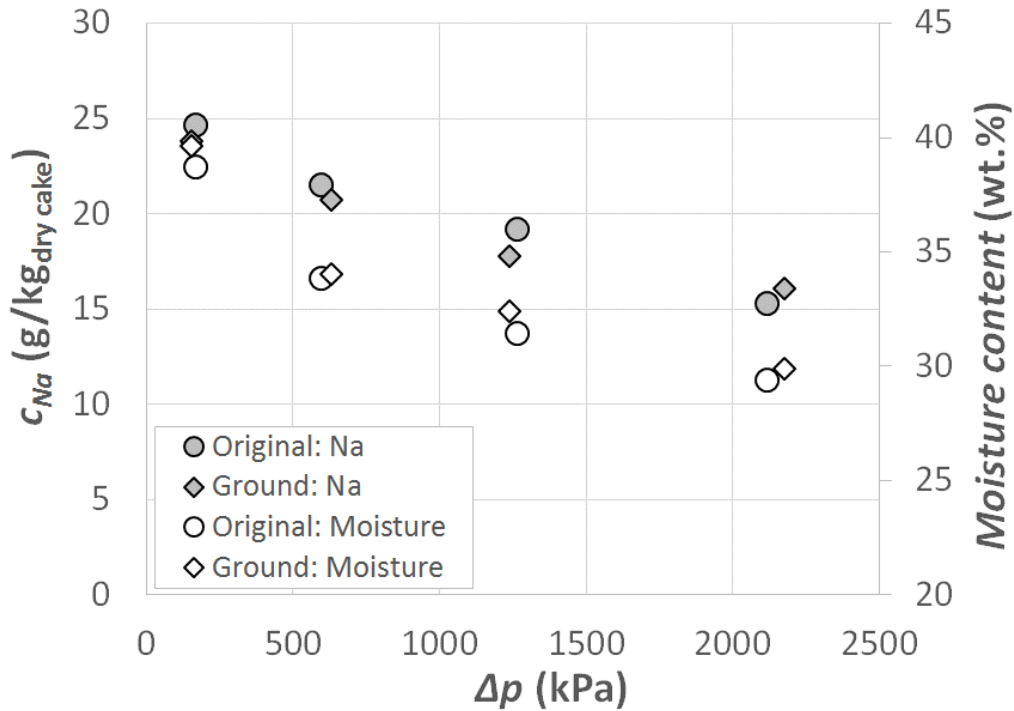
Figure 3.   Effect of filtration pressure Δp and type of slurry on the residual moisture and sodium contents of the filter cakes after compressing the cakes to terminal solidosity.

4.4.   Local pressure profiles

The local hydrostatic pressures at different heights in the filter cakes, recorded every two second, are presented in Figs. 4 and 5. Fig. 4 shows an example of the local hydrostatic pressures for the initial 1000s of filtration, while the complete pressure profiles can be found in Fig. 5. Figs. 4 and 5 show that the hydrostatic pressure within the cakes at heights of 0.5 - 12 mm above the filter medium drops rapidly after starting the filtration, due to cake formation, and decreases at a considerably slower rate after that, until the transition to the cake expression period begins.

The effect of filtration pressure on the local pressure profiles is apparent: the cake formation period preceding the point in time when the solid particles begin to carry the piston pressure and the cake expression starts, becomes shorter as the filtration pressure is increased.

The influence of particle size reduction on the local pressure profiles can also be discerned in Fig. 5. The ground slurries with finer particle size distributions (Table 1) are slightly more difficult to filter, which can be seen as extended cake formation time; also the initial expression phase following the onset of the non-linear part of the dt/dV vs. V curve to the drop of local absolute hydrostatic pressure to ambient levels, is typically somewhat extended. The relative slow hydrostatic pressure drop for both the non-ground and ground samples during the expression phase differs from what have been seen in earlier studies for cakes formed from mineral materials (e.g. [46]), indicating that expression was here notably slow for both the ground and non-ground pH-adjusted bauxite residues.

When the filtration pressure was low, the capillaries closest to the filter medium were unable to provide consistent data, as they were prone to being blocked/plugged, and therefore the data at the heights of 0.5 and 1.0 mm has been excluded in some cases.
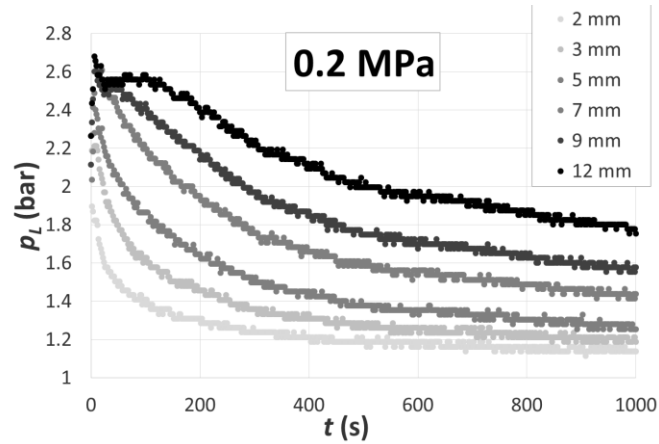

Figure 4.   Measured absolute local hydrostatic pressure profile for the initial 1000 s within the filter cell for experiments performed with the original slurry and an applied filtration pressure of 0.2 MPa.
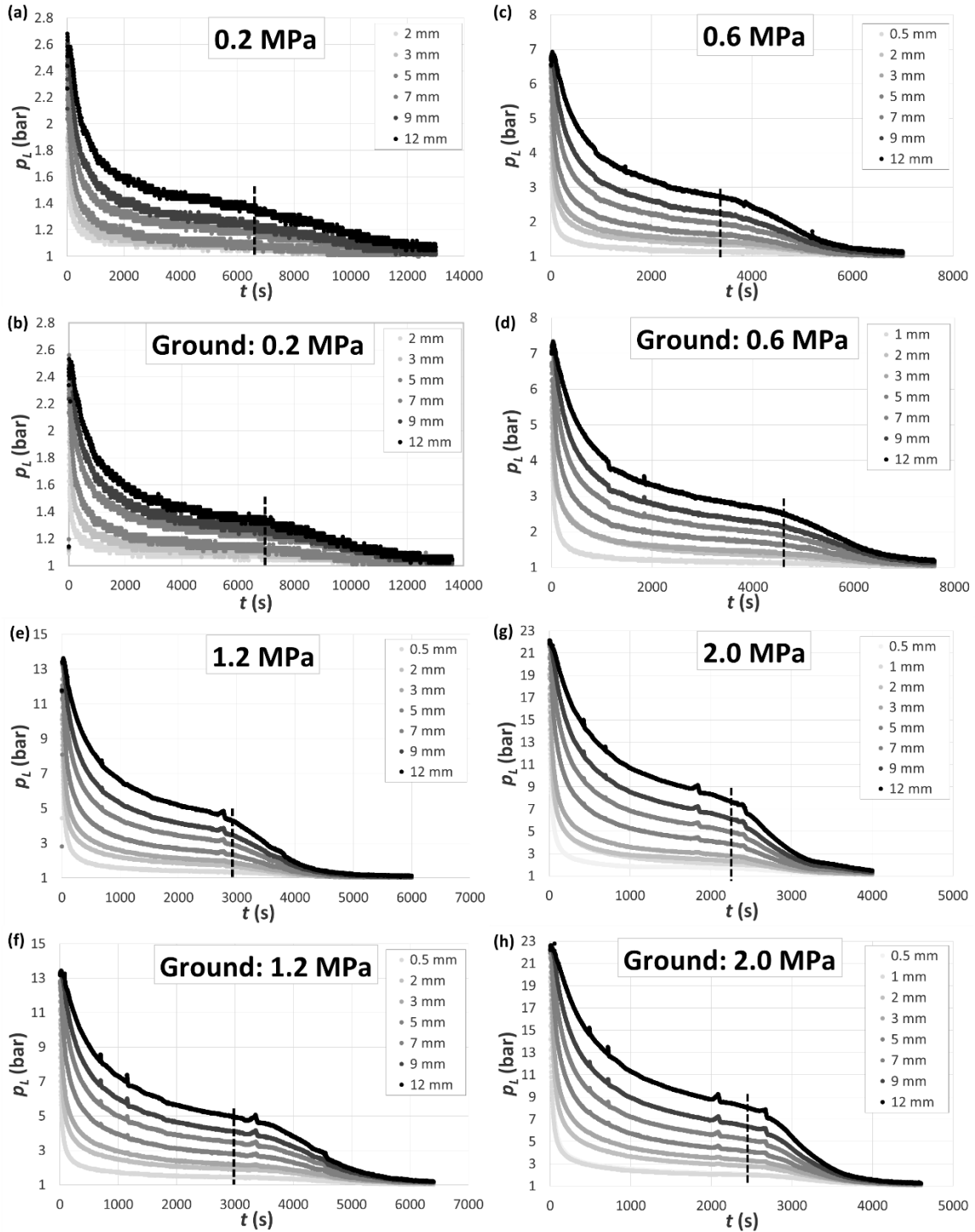
Figure 5.   Local absolute hydrostatic pressure profiles at different heights within the filter cakes for experiments performed with original and ground slurries at different filtration pressures. The dashed vertical lines indicate the end point of the cake formation period according to the end of the linear region in Fig. 1b.

4.5. *Local solidosities of the filter cakes*

Local solidosity at the height of 12 mm above the filter medium at different filtration pressures is presented in Fig. 6. The solidosities are shown for the original and ground samples during the first 10000 s of each experiment. As can be seen in Fig. 5 above, part of the cake expression period is also included in Fig. 6. The time when the hydrostatic pressure at 12 mm above the filter medium dropped to the level of ambient pressure is marked with vertical lines in Fig. 6. For experiments with 0.2 MPa filtration pressure this point was reached after approximately 12000 s for both slurries. The effect of filtration pressure on local solidosity can be seen clearly in Fig. 6 as well. Increasing the filtration pressure from 0.2 to 2 MPa increased the local solidosity at $t = 10000$ s from approximately 0.32-0.35 to 0.44-0.45.
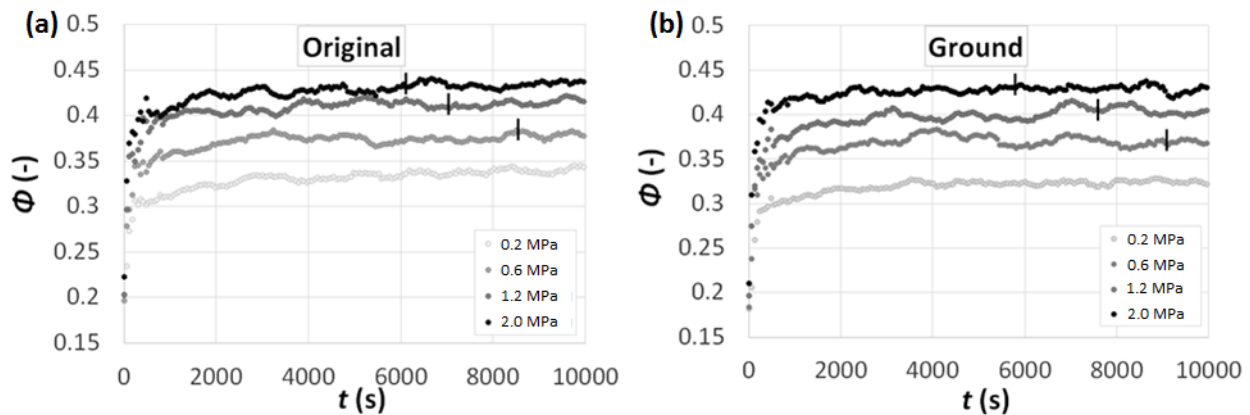

Figure 6. Local solidosity of filter cakes ($h = 12$ mm) for original (a) and ground (b) slurries at different filtration pressures. The time when the hydrostatic pressure at $h = 12$ mm became equal with the ambient pressure is indicated by vertical lines.

The local solidosity at different heights from the filter medium during constant pressure filtration at 1.2 MPa can be found in Fig. 7. These measurements show the solidosity profile during cake formation, as well as the compression of the cake yielding a more uniform solidosity profile as the cake grows higher.
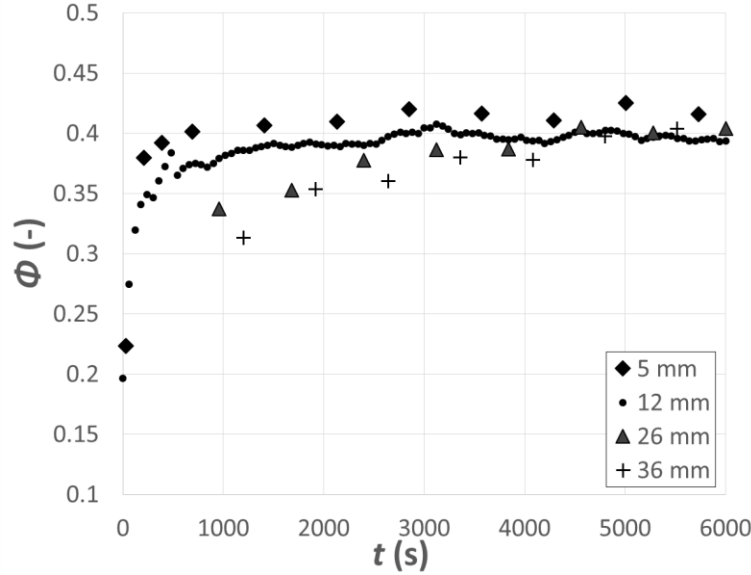
Figure 7.　Local solidosity of the filter cake formed from the ground slurry (Δp = 1.2 MPa) at four different heights above the filter medium during filtration. Data collected by i) using a constant height of measurement (h = 12 mm, Test 7) and by ii) varying the height of measurement (h = 5, 26 or 36 mm, Test 7 repeated).

Table 3 summarizes the cake heights, the terminal values of local solidosities, and the average solidosities of the cakes after compressing the cakes to constant height. The time required for this varied between 2 and 20 h, depending on the applied pressure difference, high Δp causing the fastest expression of the cake. As Table 3 shows, the obtainable terminal solidosity is a function of the filtration pressure.

Table 3.　Local solidosities Φ of the filter cakes at different heights, measured by the γ-ray attenuation method, after compressing the cakes to constant height h. The average solidosities calculated on the basis of total suspended solids and cake volume are shown for comparison.

Filtration pressure (MPa)	Type of slurry (-)	h (mm)	$\Phi_{5\,mm}$ (-)	$\Phi_{12\,mm}$ (-)	$\Phi_{26\,mm}$ (-)	$\Phi_{36\,mm}$ (-)	RSD of Φ (%)	Φ_{av} (-)
0.2	Original	98	0.35	0.33	N/A	N/A	N/A	0.32
0.6	Original	81	0.39	0.38	0.38	0.39	1.0	0.38
1.2	Original	76	0.44	0.42	0.42	0.43	2.1	0.41
2	Original	70	0.44	0.44	0.43	0.45	1.6	0.44
0.2	Ground	96	0.33	0.32	0.31	0.31	3.6	0.32
0.6	Ground	81	0.36	0.35	0.35	0.35	1.8	0.38
1.2	Ground	75	0.42	0.41	0.42	0.42	1.1	0.41
2	Ground	70	0.45	0.44	0.45	0.45	0.7	0.43

4.6.　Constitutive relationships between cake properties

The data acquired by local pressure and solidosity measurements was used for calculating the local specific cake resistance, according to Eq. (3). The local specific cake resistance, α, and local solidosity, Φ, for the filter cakes formed at 0.2-2 MPa are presented in Fig. 8a and b for experiments performed with the original slurry, and in Fig. 9a and b for those performed with the ground slurry. On the basis on Figs. 8 and 9, it can be concluded that individual experiments overlap to a good degree.
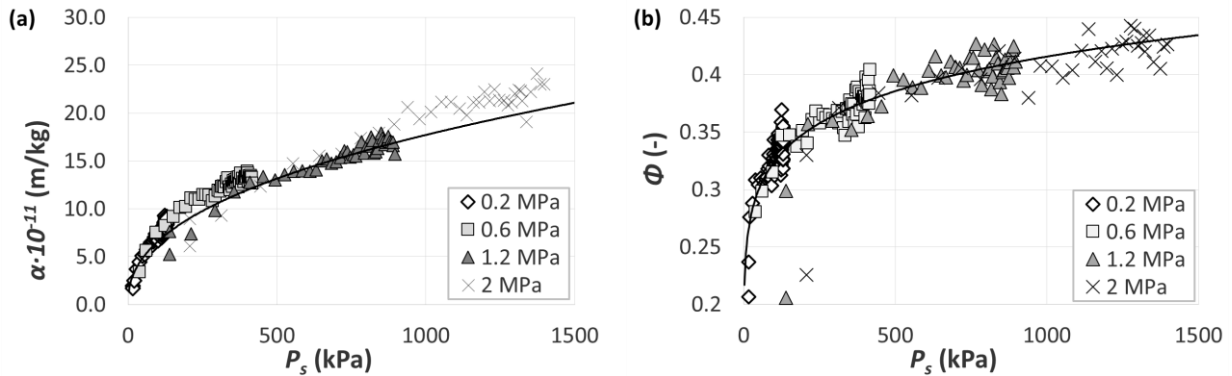

Figure 8.　　Local specific filtration resistance (a) and local solidosity (b) plotted against local solid compressive pressure for the *original* slurry at different filtration pressures. The expression period is excluded. The solid lines represents the local properties calculated from Eqs. (7) and (8) respectively according to the parameters in Table 4.
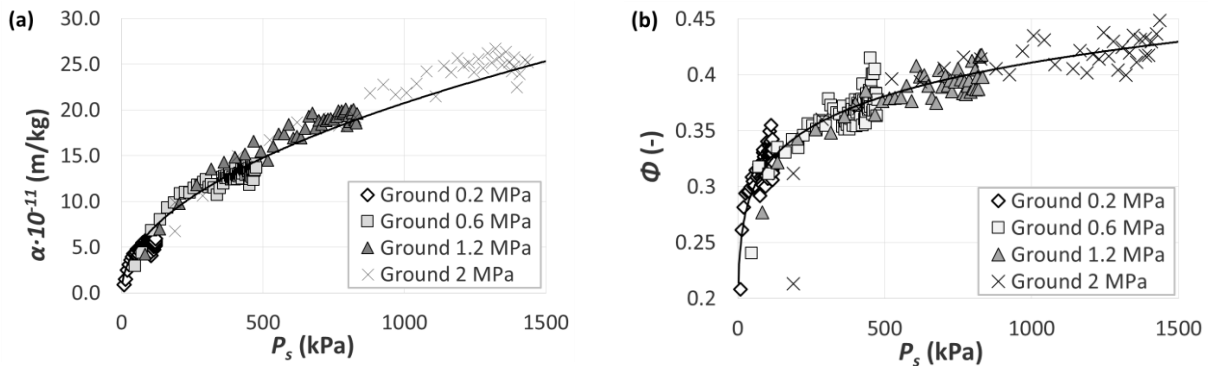

Figure 9.　　Local specific filtration resistance (a) and local solidosity (b) plotted against local solid compressive pressure for the *ground* slurry at different filtration pressures. The expression period is excluded. The solid lines represents the local properties calculated from Eqs. (7) and (8) respectively according to the parameters in Table 4.

The semi-empirical Eqs. (7) and (8) were fitted to the local data presented in Figs. 8 and 9 as well as to the average filtration resistance presented in Fig. 2, using Eq. (9). The parameter p_0 was not

fitted as it was assigned a static value (20 Pa) to facilitate comparison between the original and ground slurry. This restriction had a very limited influence on the quality of the fit. For the determination of the α_0 and n parameter Eqs. (7) and (9) was fitted to the data simultaneously, with each of the models making about the same contribution to the residual. For Eq. (9) it was assumed that the pressure drop over the cake could be approximated with the total pressure drop over the cell, this assumption can be verified from the local pressure data in Fig. 4 and 5. Fitted curves are included in the respective figures and the fitted parameters are presented in Table 4. The parameters utilized for the evaluation of compressibility with respect to α and Φ were the compressibility indices n and β, introduced in Eqs. (7) and (8), respectively. The compressibility indices n and β determined for the original and ground material suggested that both materials were slightly or moderately compressible according to the definitions presented in the literature [47,48]. The somewhat higher value of the n parameter for the cakes formed from the ground bauxite residue, 0.49, compared to 0.43 for the cakes from non-ground material, indicated that the pressure dependence of the specific cake resistance increased by the mechanical treatment. This slight increase in dependence on solid compressible pressure could not be seen for the solidosity.

Table 4.   Parameters determined from fitting Eqs. (7), (8) and (9) to the experimental data.

Type of slurry / Tests	$\alpha_0 \cdot 10^9$ (m/kg)	p_0 (Pa)	n (-)	Φ_0 (-)	β (-)
Original / 1-4	17.1	20	0.43	0.129	0.11
Ground / 5-8	10.2	20	0.49	0.126	0.11

5.   Conclusions

The local properties of pH-adjusted (pH 11) bauxite residue filter cakes were investigated. It was found that the residue formed slightly/moderately compressible filter cakes with a specific cake resistance between $5 \cdot 10^{11}$ to $1.5 \cdot 10^{12}$ m/kg for a corresponding pressure range of 0.2 to 2 MPa. The results also showed that the final cake solidosity and sodium recovery were strongly dependent on the applied pressure difference, but only to a minor extent on the particle size reduction obtained by the applied mechanical treatment. The experimental data was generally in good agreement with the applied models when semi-empirical constitutive relationships were investigated. A slight to moderate pressure dependency was found for the local cake properties, both for local specific filtration resistance and local solidosity. The filter cakes formed from mechanically treated samples displayed a somewhat higher pressure dependence for the local specific filtration resistance compared to non-ground samples. A corresponding increase of the pressure dependence could not be seen in the local solidosity of mechanically treated material. The relatively high specific cake resistance, moderate degree of compressibility of the material, and the fact that sodium recovery was enhanced with filtration pressure, make it clear that the currently applied filtration equipment, such as hyperbaric filters and filter presses, can also be recommended for the separation of bauxite residue slurries at this reduced pH.

Nomenclature

A	filtration area (m^2)
c	mass of solids in the filter cake per volume of filtrate (kg$_{dry\ solids}$/m$^3_{filtrate}$)
d_γ	inner diameter of the filter cell (m)
h	height from the filter medium (m)
n	parameter (-)
n_γ	number of counts for the filter cell with cake (-)
$n_{\gamma,0}$	number of counts for an empty filter cell (-)
Δp	pressure difference (Pa)
p_0	parameter (Pa)
p_c	pressure drop over the cake (Pa)
p_L	hydrostatic pressure (Pa)
p_s	solid compressive pressure (Pa)
R_m	resistance of the filter media (m^{-1})
RSD	relative standard deviation
t	time (s)
T	temperature (°C)
TC	total caustic
v	superficial flow velocity of the liquid in the z-direction (m/s)
V	volume of filtrate or slurry (m^3)
V_c	volume of cake (m^3)
V_{ss}	volume of suspended solids (m^3)
z	distance from the filter medium (m)

α	local specific filtration resistance (m/kg)
α_0	parameter (m/kg)
α_{av}	average specific filtration resistance (m/kg)
β	parameter (-)
μ	viscosity of the fluid (Pa s)
$\mu_{\gamma,l}$	attenuation coefficient of the liquid phase (m^{-1})
$\mu_{\gamma,s}$	attenuation coefficient of the solid phase (m^{-1})
ρ_s	solid density (kg/m^3)
Φ	local solidosity (-)
Φ_0	parameter (-)
Φ_{av}	average solidosity (-)

References

[1] C. Brunori, C. Cremisini, P. Massanisso, V. Pinto, L. Torricelli, Reuse of a treated red mud bauxite waste: studies on environmental compatibility, J. Hazard. Mater. B117 (2005) 55-63.

[2] Y. Huang, G. Han, J. Liu, W. Wang, A facile disposal of Bayer red mud based on selective flocculation desliming with organic humics, J. Hazard. Mater. 301 (2016) 46-55.

[3] M.W. Clark, M. Johnston, A.J. Reichelt-Brushett, Comparison of several different neutralisations to a bauxite refinery residue: Potential effectiveness environmental ameliorants, Appl. Geochem. 56 (2015) 1-10.

[4] M. Johnston, M.W. Clark, P. McMahon, N. Ward, Alkalinity conversion of bauxite refinery residues by neutralization, J. Hazard. Mater. 182 (2010) 710-715.

[5] M. Gräfe, C. Klauber, Bauxite residue issues: IV. Old obstacles and new pathways for in situ residue bioremediation, Hydrometallurgy 108 (2011) 46-59.

[6] M. Gräfe, G. Power, C. Klauber, Bauxite residue issues: III. Alkalinity and associated chemistry, Hydrometallurgy 108 (2011) 60-79.

[7] K. Binnemans, P.T. Jones, B. Blanpain, T. Van Gerven, Y. Pontikes, Towards zero-waste valorisation of rare-earth-containing industrial process residues: a critical review, J. Cleaner Prod. 99 (2015) 17-38.

[8] K.E. Lorber, H. Antrekowitsch, Disposal ponds and tailings dams, Waste Manag. Res. 29(2) (2011) 125-126.

[9] D. Chvedov, S. Ostap, T. Le, Surface properties of red mud particles from potentiometric titration, Colloid. Surface. A. 182 (2001) 131-141.

[10] R. Liu, C. Poon, Utilization of red mud derived from bauxite in self-compacting concrete, J. Cleaner Prod. 112 (2016) 384-391.

[11] S. Samal, A.K. Ray, A. Bandopadhyay, Proposal for resources, utilization and processes of red mud in India – a review, Int. J. Miner. Process. 118 (2013) 43-55.

[12] Y. Yang, X. Wang, M. Wang, H. Wang, P. Xian, Recovery of iron from red mud by selective leach with oxalic acid, Hydrometallurgy 157 (2015) 239-245.

[13] C.R. Borra, Y. Pontikes, K. Binnemans, T. Van Gerven, Leaching of rare earths from bauxite residue (red mud), Miner. Eng. 76 (2015) 20-27.

[14] M. Schwarz, V. Lalik, Possibilities of Exploitation of Bauxite Residue From Alumina Production. Recent Researches in Metallurgical Engineering — From Extraction to Forming. In: Nusheh, Mohammad (Ed.), InTech, 2012.

[15] V. Feigl, A. Anton, N. Uzigner, K. Gruiz, Red mud as a chemical stabilizer for soil contaminated with toxic metals, Water Air Soil Pollut. 223 (2012) 1237-1247.

[16] J. Hyun, S. Endoh, K. Masuda, H. Shin, H. Ohya, Reduction of chlorine in bauxite residue by fine particle separation, Int. J. Miner. Process. 76 (2005) 13-20.

[17] R. Milacic, T. Zuliani, J. Scancar, Environmental impact of toxic elements in red mud studied by fractionation and speciation procedures, Sci. Total Environ. 426 (2012) 359-365.

[18] T. Kinnarinen, B. Lubieniecki, L. Holliday, J. Helsto, A. Häkkinen, Enabling safe dry cake disposal of bauxite residue by deliquoring and washing with a membrane filter press, Waste Manag. Res. 33(3) (2015a) 258-266.

[19] T. Kinnarinen, B. Lubieniecki, L. Holliday, J. Helsto, A. Häkkinen, Recovery of sodium from bauxite residue by pressure filtration and cake washing, Int. J. Miner. Process. 141 (2015b) 20-26.

[20] J. Rousseaux, B. Langlois, D. Boufounos, A. Cuneo-Raffaelli, Bauxite residue filtration experience in gardanne and aluminium of Greece alumina plant. Proceedings of the 8th International Alumina Quality Workshop, Darwin, Northern Territory, Australia, 7–12 September, 2008.

[21] G. Power, M. Gräfe, C. Klauber, Bauxite residue issues: I. Current management, disposal and storage practices, Hydrometallurgy 108 (2011) 33-45.

[22] H.I. Gomes, W.M. Mayes, M. Rogerson, D.I. Stewart, I.T. Burke, Alkaline residues and the environment: a review of impacts, management practices and opportunities, J. Cleaner Prod. 112 (2016) 3571-3582.

[23] D.J. Cooling, Improving sustainability of residue management practices – Alcoa World Alumina Australia. Paste 2007 – A. Fourie and R.J. Jewell (eds). Australian centre for geomechanics, Perth, Australia, 2007.

[24] L.J. Kirwan, A. Hartshorn, J.B. McMonagle, L. Fleming, D. Funnell, Chemistry of bauxite residue neutralisation and aspects to implementation, Int. J. Miner. Process. 119 (2013) 40-50.

[25] H. P. G. Darcy, Les Fontaines Publiques de la Ville de Dijon. Victor Dalamont, Paris, 1856.

[26] T. Mattsson, M. Sedin, H. Theliander, On the local filtration properties of microcrystalline cellulose during dead-end filtration, Chem. Eng. Sci. 72 (2012) 51-60.

[27] G.G. Chase, M.S. Willis, Compressive cake filtration, Chem. Eng. Sci. 47(6) (1992) 1373-1381.

[28] M. Shirato, T. Aragaki, K. Ichimura, N. Ootsuji, Porosity variation in filter cake under constant-pressure filtration, J. Chem. Eng. Japan 4(2) (1971) 60-65.

[29] S. Okamura M. Shirato, Liquid pressure distribution within cakes in the constant pressure filtration, Kagaku Kogaku 19(111) (1955) 104-110.

[30] C. Johansson, H. Theliander, Measuring concentration and pressure profiles in dead-end filtration, Filtration 3(2) (2003) 114-120.

[31] G.H. Meeten, A dissection method for analysing filter cakes, Chem. Eng. Sci. 48(13) (1993) 2391-2398.

[32] C.C. Dell, J. Sinha, The mechanism of removal of water from flocculated clay sediments, Trans. Br. Ceram. Soc. 63 (1964) 603-614.

[33] M.A. Horsfield, E.J. Fordham, C. Hall, L.D. Hall, 1H NMR Imaging studies of filtration in colloidal suspensions, J. Magn. Reson. 81 (1989) 593-596.

[34] E.J. La Heij, P. J. A. M Kerkhof, K. Kopinga, L. Pel, Determining porosity profiles during filtration and expression of sewage sludge by NMR imaging, AIChE J. 42(4) (1996) 953-959.

[35] B.R. Bierck, S.A. Wells, R.I. Dick, Compressible cake filtration: monitoring cake formation and shrinkage using synchrotron x-rays, Journal WPCF 60(5) (1988) 645-650.

[36] F.M. Tiller, N.B. Hsyung, D.Z. Cong, Role of porosity in filtration: XII. Filtration with sedimentation, AIChE J. 41(5) (1995) 1153-1164.

[37] A.J.P. Borges, R.A. Hauser-Davis, T.F. de Oliveira, Cleaner red mud residue production at an alumina plant by applying experimental design techniques in the filtration stage, J. Cleaner Prod. 19 (2011) 1763-1769.

[38] M. Miranda de Castro, R. Wischnewski, L.G. Correa, J.R.A. Filho, A new concept for dry disposal of Alunorte's bauxite residue. Proceedings of the 9th International Alumina Quality Workshop, 2012.

[39] T. Kinnarinen, R. Tuunila, M. Huhtanen, A. Häkkinen, P. Kejik, T. Sverak, Wet grinding of $CaCO_3$ with a stirred media mill: Influence of obtained particle size distributions on pressure filtration properties, Powder Technol. 273 (2015c) 54-61.

[40] S.P. Usher, Suspension dewatering: characterisation and optimisation. Ph.D. Thesis, University of Melbourne, Victoria, Australia, 2002.

[41] C. Johansson, H. Theliander, Validation of predicted local profiles in cake filtration, Tran IchemE 85(A2) (2007) 220-228.

[42] M. Shirato, M. Sambuichi, H. Kato, T. Aragaki, Internal flow mechanism in filter cakes, AIChE J. 15(3) (1969) 405–409.

[43] T. Mattsson, M. Sedin, H. Theliander, Zeta-potential and local filtration properties: Constitutive relationships for TiO_2 from experimental filtration measurements, Chem. Eng. Sci. 66 (2011) 4573-4581.

[44] S. Ripperger, W. Gösele, C. Alt, Filtration, Ullmann's Encyclopedia of Industrial Chemistry, Fundamentals, 1,Wiley-VCH Verlag GmbH & Co. KgaA, Weinheim, 2012.

[45] F.M. Tiller, W.F. Leu, Basic data fitting in filtration, J. Chin. Inst. Chem. Eng. 11 (1980) 61-70.

[46] P. Sedin, C. Johansson, H. Theliander, On the measurement and evaluation of pressure and solidosity in filtration, Trans. IchemE. 81A (2003) 1393-1405.

[47] F.M. Tiller, L.L. Horng, Hydraulic deliquoring of compressible filter cakes. Part 1: Reverse flow in filter presses, AIChE J. 29(2) (1983) 297-305.

[48] M. Oja, Pressure filtration of mineral slurries: Modelling and particle shape characterization. Doctoral thesis, Lappeenranta University of Technology, Lappeenranta, Finland, 1996.